

Decentralized Robust Energy Management of Multi-area Integrated Electricity-gas Systems

Nan Jia, *Student Member, IEEE*, Cheng Wang, *Member, IEEE*, Wei Wei, *Senior Member, IEEE*, and Tianshu Bi, *Senior Member, IEEE*

Abstract—This paper proposes a fast and decentralized solution methodology for the robust operation of multi-area integrated electricity-gas systems (M-IEGSs). A deterministic reformulation is obtained for the two-stage robust model by applying the linear decision rule based electrical reserve utilization scheme as well as regulating the distributed gas storages. Two linear approximations are developed for the nonconvex Weymouth equation in the gas network to determine the gas flow directions. The penalty convex-concave procedure (P-CCP) is then adopted to refine a feasible local optimum for the nonconvex model with an acceleration strategy. The decentralized decision-making is enabled by the alternating direction multipliers method (ADMM). The convergence as well as computation performance of the overall solution procedure can be guaranteed as only convex optimizations are solved. Simulation results validate the effectiveness of the proposed methods as well as the benefits of the proposed convex programming based solution procedure.

Index Terms—Convex optimization, decentralized robust optimization, energy management, linear approximation, integrated electricity-gas system.

NOMENCLATURE

A. Indices and Sets

$\mathcal{A}_i^e, \mathcal{A}_i^g$	Areas connecting to area i by tie-line and tie-pipeline
$c \in \mathcal{C}$	Gas compressor
c^+, c^-	Initial and terminal nodes of compressor
$\mathcal{C}^+(n_g)$	Compressor whose initial node is n_g
$\mathcal{C}^-(n_g)$	Compressor whose terminal node is n_g
$d_e \in \mathcal{D}_e$	Electrical load
$d_g \in \mathcal{D}_g$	Gas load
$\mathcal{D}_g(n_g)$	Gas load connected to node n_g

$\mathcal{D}_g(s)$	Gas load connected to gas storage (GS)
$i, j \in \mathcal{A}$	Areas
$l_e \in \mathcal{L}_e$	Power transmission line
$l_p \in \mathcal{L}_p$	Gas network pipeline
l_p^+, l_p^-	Initial and terminal nodes of pipeline l_p
$\mathcal{L}_p^+(n_g)$	Pipeline whose initial node is n_g
$\mathcal{L}_p^-(n_g)$	Pipeline whose terminal node is n_g
$n_e \in \mathcal{N}_e$	Power network bus
$n_g \in \mathcal{N}_g$	Gas network node
$s \in \mathcal{S}$	GS
$\mathcal{S}(n_g)$	GS connected to node n_g
$t, t' \in \mathcal{T}$	Time periods
$u \in \mathcal{U}_N \cup \mathcal{U}_G$	Union of non-gas fired unit (NGU) and gas-fired unit (GU)
$u_G \in \mathcal{U}_G$	GU
$\mathcal{U}_G(s)$	GU connected to GS s
$u_R \in \mathcal{U}_R$	Renewable generation unit (RGU)
$u_N \in \mathcal{U}_N$	NGU
$w \in \mathcal{W}$	Gas well (GW)
$\mathcal{W}(n_g)$	GW connected to node n_g

B. Parameters

Ψ_{l_p}	Weymouth equation coefficient
$\tau_{n_g}^{\max}, \tau_{n_g}^{\min}$	The maximum and minimum limits of nodal pressure square
λ_c	Gas consumption rate of compressors
$\eta_s^{\text{in}}, \eta_s^{\text{out}}$	Input and output efficiencies of GS
η_{u_G}	Gas-to-power efficiency of GU
A, b, A^*, b^*	Constant matrices and vectors
A_e, B_e, c_e	Constant matrices and vectors of tie-line constraints among regional integrated electricity-gas systems (R-IEGSs)
A_g, B_g, c_g	Constant matrices and vectors of tie-pipeline constraints among R-IEGSs
$c_{u_N}^0, c_{u_N}^1, c_{u_N}^2$	Constant, linear, and quadratic cost coefficients of NGU outputs
$c_{u_N}^{\text{up}}, c_{u_N}^{\text{down}}$	Cost coefficients of upward reserve (UR) and downward reserve (DR) of NGU
c_w	Cost coefficient of GW

Manuscript received: February 28, 2020; accepted: August 3, 2020. Date of CrossCheck: August 3, 2020. Date of online publication: February 17, 2021.

This work was supported by Science and Technology Project of State Grid Corporation of China (No. SGJX0000KXJS1900321).

This article is distributed under the terms of the Creative Commons Attribution 4.0 International License (<http://creativecommons.org/licenses/by/4.0/>).

N. Jia, C. Wang (corresponding author), and T. Bi are with the State Key Laboratory of Alternate Electrical Power System with Renewable Energy Sources, North China Electric Power University, Beijing, China (e-mail: jianan96dqc@163.com; chengwang@ncepu.edu.cn; tsbi@ncepu.edu.cn).

W. Wei is with the Department of Electrical Engineering, Tsinghua University, Beijing, China (e-mail: wei-wei04@mails.tsinghua.edu.cn).

DOI: 10.35833/MPCE.2020.000112



c_s^{up}, c_s^{down}	Cost coefficients of UR and DR of GS
d_e, d_g	Lagrangian constants of coupling constraints
$F_{d_e t}$	Predicted value of gas load
$F_{s, \max}^{out}, F_{s, \min}^{out}$	The maximum and minimum output flow of GS
F_w^{\max}, F_w^{\min}	The maximum and minimum output of GW
G_{ul_e}	Generation shift distribution factor (GSDF) of NGU and GU
$G_{u_R l_e}, G_{d_e l_e}$	GSDFs of RGU output and electrical load
G_{jl_e}	GSDF of tie-line with area j
K	Heating value of gas
$P_{d_e t}, P_{u_R t}$	Predicted values of electrical load and RGU output
$P_{ij}^{\max}, F_{ij}^{\max}$	The maximum power of tie-line and tie-pipeline
$P_{l_e}^{\max}$	Capacity of transmission line
P_u^{\max}, P_u^{\min}	The maximum and minimum values of NGU and GU
Q, q, r	Constant matrices and vectors of objective function
Re_u^{up}, Re_u^{down}	Ramping rates of NGU and GU
S_s^{ini}	Initial stored gas of GS
S_s^{\max}, S_s^{\min}	The maximum and minimum capacities of GSs
Z_c	The maximum compression rate of compressor
$[\Delta F_{d_e t}^{\min}, \Delta F_{d_e t}^{\max}]$	Interval of gas load uncertainty
$[\Delta f_{st}^{\min}, \Delta f_{st}^{\max}]$	Flow interval of GS
$\Delta f_{st}^{out}, \Delta f_{st}^{in}$	Gas flow adjustment of output and input of GS
Δp_{ut}	Adjustment of NGU and GU outputs
$[\Delta P_{d_e t}^{\min}, \Delta P_{d_e t}^{\max}]$	Interval of electrical load uncertainty
C. Decision Variables	
α_{ut}	RPF of NGU or GU
$\alpha_{u_R t}, \alpha_{u_G t}$	RPFs of NGUs and GUs
$\tau_{n_g t}$	Nodal pressure square
$\tau_{p_t}^+, \tau_{p_t}^-$	Initial and terminal pressure squares of pipeline
$\tau_{c^+ t}, \tau_{c^- t}$	Initial and terminal pressure squares of compressor
$\phi_{l_e u_R t}, \phi'_{l_e u_R t}$	Instrumental variables
$\phi_{l_e d_e t}, \phi'_{l_e d_e t}$	
$\xi_{p_t}^k$	Slack variable at the k^{th} iteration of P-CCP
$Cost_i(x_i)$	Objective function of R-IEGS i
$f_{st}^{in}, f_{st}^{out}$	Input and output flows of GSs
$f_{l_e t}$	Flow of pipeline
$f_{l_e t}^0$	Initial flow of pipeline
f_{ct}^+, f_{ct}^-	Input and output flows of compressors
f_{wt}	Gas production of GW
p_{ut}	Output of NGU and GU

p_i^{ij}, f_i^{ij}	Power and gas flow from areas i to j
$p_{l_e t}$	Power of line with uncertainty
$p_{l_e t}^0$	Power of line without uncertainty
$r_{ut}^{up}, r_{ut}^{down}$	UR and DR of NGU and GU
S_{st}	Gas reserve of GS
λ_e, λ_g	Dual variables of the coupling constraints among R-IEGSs
x	Vector of decision variables
$x_i \in \Omega_i$	Vector of decision variables in R-IEGS i
D. Random Variables	
$\Delta \tilde{f}_{d_e t}$	Gas load deviation
\tilde{f}_{st}	Gas flow of GS in random cases
$\Delta \tilde{p}_{u_R t}, \Delta \tilde{p}_{d_e t}$	Deviations of RGU output and electrical load
$\tilde{p}_{u_G t}, \tilde{p}_{u_N t}$	Power of GU and NGU in random cases
$\tilde{p}_{l_e t}$	Power of line in random cases
\tilde{S}_{st}	Gas reserve of GS in random cases

I. INTRODUCTION

IN recent years, influenced by the remarkable drop of natural gas prices [1], the proportion of natural gas in the total energy consumption rises rapidly. Compared with coal-fired units, natural gas-fired units (GUs) have the advantages of rapid dynamic characteristics and low emission, and are deployed gradually in power network [2]. With the growing share of GUs among controllable generation assets, the emerging power-to-gas technologies [3], and the integrated demand response [4], not only the physical interdependencies between power and gas systems have been enhanced, but also a new research topic, i.e., the integrated electricity-gas system (IEGS) has emerged [5], [6]. With the broad participation of diverse energy suppliers, a whole IEGS typically consists of several regional-IEGSs (R-IEGSs) owned by different operators, namely multi-area IEGSs (M-IEGSs), and the interconnection of several R-IEGSs is beneficial to the improvement of security and feasibility [7]. In view of the information privacy of operators, a decentralized optimization of M-IEGSs becomes an urgent need.

Alternating direction multipliers method (ADMM) serves as a decentralized optimization method [8] and has been widely adopted in the optimization of power system [9], where the model convexity is required to ensure the convergence of the algorithm. However, due to the existence of the nonconvex and nonlinear Weymouth equation in the gas system operation model, the decentralized optimization of M-IEGSs becomes challenging. Quite a few inspiring works have been carried out on dealing with the Weymouth equation. To provide tractable formulations for the commercial solvers, [10]-[13] adopt the piecewise linearization method to approximate the Weymouth equation, transforming the original nonlinear programs (NLPs) to mixed-integer linear programs (MILPs). To avoid additional computation burden brought by the auxiliary integer variables, [14] adopts the second-order cone (SOC) relaxation to tackle the Weymouth

equation, where the gas flow directions are assumed to be fixed. Based on the work of [14], the penalty-convex-concave process (P-CCP) is adopted in [15] to drive the infeasible solution to a feasible one. Notably, similar solution feasibility recovery methods can be found in [16], [17].

In practice, the gas flow directions may not be fixed, especially when the topology of the gas network is non-radial or looped. Along this line, a binary variable is introduced for each Weymouth equation to represent the gas flow direction, and the overall model would become a mixed-integer SOC program (MISOCP) in [18] and [19] after performing the mixed-integer SOC relaxation. To enhance the tightness of the relaxation, P-CCP is adopted in [18], where a heuristic method is proposed to improve the convergence of P-CCP. The big- M method is adopted in [20] to transform the NLP to an MISOCP, then a multi-slack-node gas flow calculation method based on the Newton-Raphson algorithm is proposed to enhance the relaxation tightness. Similar to the SOC relaxation method, a series of linear segments are used to envelope SOC region through the first-order Taylor series expansion of Weymouth equation in [21], [22], whereas the relaxation tightness is unconsidered.

In addition to the internal difficulty in dealing with the operation model of gas systems, the uncertainties of external renewable energy generation have also imposed great challenges on the operation of IEGSs, giving rise to urgent demands for the robust optimization method of IEGS. Reference [23] proposes a robust energy management framework for IEGSs against a set of predetermined scenarios of wind generation outputs. The interval-based wind generation uncertainty set is adopted in [24], [25], where a robust dispatch strategy can be obtained for IEGSs considering demand response schemes.

The aforementioned works contribute to the robust optimization of IEGS, whereas only a few of them focus on the decentralized robust optimization. The application scenarios of decentralized robust optimization in the existing works can be divided into two categories. One targets at analyzing the interactions between power and gas networks [12], and the other is designed for coordinating multiple interconnected R-IEGSs [18]. As mentioned above, nonconvex programs with binary variables such as MILP and MISOCP are used for the optimization of IEGS in the existing works, which challenge the convergence of ADMM. In this regard, [12] proposes a tailored ADMM, whose essence is to separate the process of decentralized robust optimization and the computation of binary variables. Similar to [12], [18] proposes an iterative ADMM to realize the decentralized robust optimization of M-IEGSs. In order to better understand the aforementioned works and provide a list of research gaps, the contrastive review is introduced in Table I.

This paper aims at the decentralized optimization of M-IEGSs from the perspective of eliminating nonconvexity of Weymouth equation, and a fast calculation method for the decentralized robust optimization strategy of M-IEGSs is proposed. The interval-based uncertainty modeling as well as linear-decision-rule (LDR) based recourse action mechanism is adopted for the robust energy management of M-IEGSs. Two novel linear approximations for nonconvex Weymouth

equation are derived to determine the directions as well as initial solutions of gas flow. Then, P-CCP is adopted to recover solution feasibility, where an acceleration method is proposed to reduce the computation complexity. The decentralized optimization of M-IEGSs is achieved by ADMM. Compared with the existing literature, the salient features of this work are summarized as follows.

TABLE I
CONTRASTIVE REVIEW OF AFOREMENTIONED WORKS

Reference	Unfixed gas flow direction	Decentralized optimization	Robust optimization	Convexity of model
[11], [17]	√	×	×	×
[12]	√	√	√	×
[14], [16], [21]	×	×	√	√
[15]	×	√	×	√
[18]	√	√	×	×
[13], [20], [23], [24]	√	×	√	×
[22]	√	×	√	√

Note: “√” represents that the item is satisfied; “×” represents that the item is not satisfied.

1) Two linear approximations for the nonconvex Weymouth equation are proposed, which are used for determining the gas flow directions without introducing binary variables. The impacts of the proposed approximation methods on the feasible region of the original problem are analyzed through the mapping between the pressure squares of the initial and terminal nodes of a pipeline.

2) A convex programming based decentralized solution procedure is designed for the proposed M-IEGS robust energy management problem, where the gas flow directions and the infeasibility issues in the Weymouth equations resulting from constraint relaxation are tackled sequentially, based on the idea of divide-and-conquer. The solutions among different R-IEGSs are coordinated through the ADMM algorithm, whose convergence can be guaranteed by the convexity of the reformulated model.

3) Through the designed solution procedure, an optimal or feasible solution can be obtained at least. And the solution acceleration is achieved via preferentially mitigating the Weymouth equation infeasibility in the local gas network. Simulation results show that the designed solution procedure could reduce computation time compared with existing references, especially for large-scale cases.

II. MATHEMATICAL FORMULATION

The studied M-IEGSs include several R-IEGSs, each of which is tied by power transmission lines, gas pipelines, and communication facilities. GUs are served as coupling elements for power and gas networks.

A. Objective Function

The objective (1) is to minimize the total energy consumption and reserve costs of R-IEGS i . The reserve is used to mitigate the uncertainty of renewable generation units

(RGUs) and loads.

$$\begin{aligned} Cost_i = \min & \left\{ \sum_{t \in \mathcal{T}} \sum_{u_N \in \mathcal{U}_N} (c_{u_N}^0 + c_{u_N}^1 p_{u_N t} + c_{u_N}^2 p_{u_N t}^2) + \right. \\ & \sum_{t \in \mathcal{T}} \sum_{u_N \in \mathcal{U}_N} (c_{u_N}^{up} r_{u_N t}^{up} + c_{u_N}^{down} r_{u_N t}^{down}) + \sum_{t \in \mathcal{T}} \sum_{w \in \mathcal{W}} c_w f_{wt} + \\ & \left. \sum_{t \in \mathcal{T}} \sum_{s \in \mathcal{S}} \left(\frac{c_s^{up} \Delta f_{st}^{max}}{\eta_s^{out}} - c_s^{down} \Delta f_{st}^{min} \eta_s^{in} \right) \right\} \quad (1) \end{aligned}$$

B. Constraint of IEGS

In the model of IEGS, the uncertainties of RGUs and loads are considered as (2)-(4) [20], and the uncertainty interval can be determined according to the prediction accuracy.

$$\Delta P_{u_R t}^{min} \leq \Delta \tilde{p}_{u_R t} \leq \Delta P_{u_R t}^{max} \quad \forall u_R, \forall t \quad (2)$$

$$\Delta P_{d_e t}^{min} \leq \Delta \tilde{p}_{d_e t} \leq \Delta P_{d_e t}^{max} \quad \forall d_e, \forall t \quad (3)$$

$$\Delta F_{d_g t}^{min} \leq \Delta \tilde{f}_{d_g t} \leq \Delta F_{d_g t}^{max} \quad \forall d_g, \forall t \quad (4)$$

In the power network, the DC power flow mode is adopted [11], [12], [22], and the base-case constraints without uncertainties are shown as (5)-(8). Particularly, (5) and (6) are the whole network power balancing condition and power flow constraint of transmission lines, respectively. Formulae (7) and (8) show the power and ramping constraints of NGUs and GUs, respectively. When the actual outputs of RGUs and electrical loads deviate from the predicted values, the outputs of NGUs and GUs should be adjusted accordingly. However, the power flow of tie-line would not be adjusted since its value has been determined in day-ahead mode [26]. The operation constraints of the power network considering uncertainties are shown as (9)-(14). Particularly, the whole network power balancing condition is shown in (9), and (10) expresses the adjustment limits of NGUs and GUs [27], including upward reserves (URs) and downward reserves (DRs), whose constraints are introduced in (11). Formulae (12) and (13) show the power and ramping constraints of NGUs and GUs, respectively. Formula (14) depicts the power flow constraint of transmission lines.

$$\sum_{u \in \mathcal{U}_N \cup \mathcal{U}_G} p_{ut} + \sum_{u_R \in \mathcal{U}_R} P_{u_R t} - \sum_{j \in \mathcal{A}_i^e} p_t^{ij} - \sum_{d_e \in \mathcal{D}_e} P_{d_e t} = 0 \quad \forall t \quad (5)$$

$$\begin{aligned} -P_{l_e}^{max} \leq p_{l_e t} = & \sum_{u \in \mathcal{U}_N \cup \mathcal{U}_G} G_{u l_e} p_{ut} + \sum_{u_R \in \mathcal{U}_R} G_{u_R l_e} P_{u_R t} - \\ & \sum_{j \in \mathcal{A}_i^e} G_{j l_e} p_t^{ij} - \sum_{d_e \in \mathcal{D}_e} G_{d_e l_e} P_{d_e t} \leq P_{l_e}^{max} \quad \forall l_e, \forall t \quad (6) \end{aligned}$$

$$P_u^{min} \leq p_{ut} \leq P_u^{max} \quad \forall u, \forall t \quad (7)$$

$$-Re_u^{down} \leq p_{ut} - p_{u(t-1)} \leq Re_u^{up} \quad \forall u, \forall t \quad (8)$$

$$\begin{aligned} \sum_{u \in \mathcal{U}_N \cup \mathcal{U}_G} (p_{ut} + \Delta p_{ut}) + \sum_{u_R \in \mathcal{U}_R} (P_{u_R t} + \Delta \tilde{p}_{u_R t}) - \sum_{j \in \mathcal{A}_i^e} p_t^{ij} - \\ \sum_{d_e \in \mathcal{D}_e} (P_{d_e t} + \Delta \tilde{p}_{d_e t}) = 0 \quad \forall t \quad (9) \end{aligned}$$

$$-r_{ut}^{down} \leq \Delta p_{ut} \leq r_{ut}^{up} \quad \forall u, \forall t \quad (10)$$

$$\begin{cases} r_{ut}^{down} \geq 0 \\ r_{ut}^{up} \geq 0 \end{cases} \quad \forall u, \forall t \quad (11)$$

$$P_u^{min} \leq p_{ut} + \Delta p_{ut} \leq P_u^{max} \quad \forall u, \forall t \quad (12)$$

$$-Re_u^{down} \leq (p_{ut} + \Delta p_{ut}) - (p_{u(t-1)} + \Delta p_{u(t-1)}) \leq Re_u^{up} \quad \forall u, \forall t \quad (13)$$

$$\begin{aligned} -P_{l_e}^{max} \leq & \sum_{u \in \mathcal{U}_N \cup \mathcal{U}_G} G_{u l_e} (p_{ut} + \Delta p_{ut}) + \sum_{u_R \in \mathcal{U}_R} G_{u_R l_e} (P_{u_R t} + \Delta \tilde{p}_{u_R t}) - \\ & \sum_{j \in \mathcal{A}_i^e} G_{j l_e} p_t^{ij} - \sum_{d_e \in \mathcal{D}_e} G_{d_e l_e} (P_{d_e t} + \Delta \tilde{p}_{d_e t}) = p_{l_e t} \leq P_{l_e}^{max} \quad \forall l_e, \forall t \quad (14) \end{aligned}$$

In the gas network, the base-case operation constraints are shown as (15)-(23). Formulae (15) and (16) describe the limits of GW outputs and nodal pressure square, respectively. In this work, the steady-state gas flow model is employed, which is similar to [18] - [20]. Therefore, the steady-state Weymouth equation is presented in (17) without linepack [10], which depicts the relationship between the gas flow in pipeline and the nodal pressure squares. A simplified compressor model is introduced in (18) and (19) [18], [20]. The nodal gas balancing condition is given in (20) with linear GU model [14], [20], and the operation constraints of GSs are described by (21)-(23). Specifically, (21) is imposed to limit input and output flows of GSs in the worst case, (22) is added to guarantee the limit of available gas, and (23) sets initial stored gas for GSs. To mitigate the uncertainties in the gas network, the outputs of GSs would be adjusted. Equation (24) shows the nodal gas balancing condition considering uncertainties, and (25) and (26) express the operation limits of GSs. It should be noted that the uncertainty in the gas network mainly comes from two aspects, which are the inherent gas load uncertainty and the gas demand uncertainty of the GUs.

$$F_w^{min} \leq f_{wt} \leq F_w^{max} \quad \forall w, \forall t \quad (15)$$

$$\tau_{n_g}^{min} \leq \tau_{n_g t} \leq \tau_{n_g}^{max} \quad \forall n_g, \forall t \quad (16)$$

$$f_{l_p t} \left| f_{l_p t} \right| = \psi_{l_p} (\tau_{l_p t} - \tau_{l_p t}) \quad \forall l_p, \forall t \quad (17)$$

$$\tau_{c_t} \leq Z_c^2 \tau_{c_t} \quad f_{ct}^+ \geq 0, \forall c, \forall t \quad (18)$$

$$f_{ct}^- = (1 - \lambda_c) f_{ct}^+ \quad \forall c, \forall t \quad (19)$$

$$\begin{aligned} \sum_{w \in \mathcal{W}(n_g)} f_{wt} + \sum_{s \in \mathcal{S}(n_g)} (f_{st}^{out} - f_{st}^{in}) - \sum_{l_p \in \mathcal{L}_p^+(n_g)} f_{l_p t} + \sum_{l_p \in \mathcal{L}_p^-(n_g)} f_{l_p t} - \\ \sum_{c \in \mathcal{C}^+(n_g)} f_{ct}^+ + \sum_{c \in \mathcal{C}^-(n_g)} f_{ct}^- - \sum_{j \in \mathcal{A}_i^e(n_g)} f_t^{ij} - \sum_{d_g \in \mathcal{D}_g(n_g)} F_{d_g t} - \sum_{u_G \in \mathcal{U}_G(n_g)} \frac{P_{u_G t}}{\eta_{u_G}} K = 0 \quad \forall n_g, \forall t \quad (20) \end{aligned}$$

$$\begin{cases} 0 \leq f_{st}^{in} \leq F_{s, max}^{in} \\ 0 \leq f_{st}^{out} \leq F_{s, max}^{out} \end{cases} \quad \forall s, \forall t \quad (21)$$

$$S_s^{min} \leq s_{st} = s_{s(t-1)} + f_{st}^{in} \eta_s^{in} - \frac{f_{st}^{out}}{\eta_s^{out}} \leq S_s^{max} \quad \forall s, \forall t \quad (22)$$

$$s_{s(t=T)} = s_{s(t=1)} = S_s^{ini} \quad \forall s \quad (23)$$

$$\begin{aligned} \sum_{w \in \mathcal{W}(n_g)} f_{wt} + \sum_{s \in \mathcal{S}(n_g)} (f_{st}^{out} + \Delta f_{st}^{out} - f_{st}^{in} - \Delta f_{st}^{in}) - \sum_{l_p \in \mathcal{L}_p^+(n_g)} f_{l_p t} + \\ \sum_{l_p \in \mathcal{L}_p^-(n_g)} f_{l_p t} - \sum_{c \in \mathcal{C}^+(n_g)} f_{ct}^+ + \sum_{c \in \mathcal{C}^-(n_g)} f_{ct}^- - \sum_{j \in \mathcal{A}_i^e(n_g)} f_t^{ij} - \\ \sum_{d_g \in \mathcal{D}_g(n_g)} (F_{d_g t} + \Delta \tilde{f}_{d_g t}) - \sum_{u_G \in \mathcal{U}_G(n_g)} \frac{p_{u_G t} + \Delta \tilde{p}_{u_G t}}{\eta_{u_G}} K = 0 \quad \forall n_g, \forall t \quad (24) \end{aligned}$$

$$\begin{cases} 0 \leq f_{st}^{in} + \Delta f_{st}^{in} \leq F_{s,max}^{in} \\ 0 \leq f_{st}^{out} + \Delta f_{st}^{out} \leq F_{s,max}^{out} \end{cases} \quad \forall s, \forall t \quad (25)$$

$$S_s^{min} \leq \tilde{s}_{st} = \tilde{s}_{s(t-1)} + (f_{st}^{in} + \Delta f_{st}^{in})\eta_s^{in} - \frac{f_{st}^{out} + \Delta f_{st}^{out}}{\eta_s^{out}} \leq S_s^{max} \quad \forall s, \forall t \quad (26)$$

Besides the aforementioned local operation constraints, the capacity constraints need to be considered for the DC tie-lines and gas tie-pipelines, where the gas flows are assumed to be full controllable [18]. Formulae (27) and (28) present the coordination and capacity constraints of DC tie-lines and gas tie-pipelines, respectively.

$$\begin{cases} p_t^{ij} + p_t^{ji} = 0 \\ -P_{ij}^{max} \leq p_t^{ij} \leq P_{ij}^{max} \end{cases} \quad \forall i, \forall j \in \mathcal{A}_i^e, \forall t \quad (27)$$

$$\begin{cases} f_t^{ij} + f_t^{ji} = 0 \\ -F_{ij}^{max} \leq f_t^{ij} \leq F_{ij}^{max} \end{cases} \quad \forall i, \forall j \in \mathcal{A}_i^g, \forall t \quad (28)$$

C. Linear Decision Rule Based Uncertainty Mitigation Scheme

For the deviations of RGUs and electrical loads with respect to the predicted values, the output power of NGUs and GUs should be adjusted accordingly. Here, a LDR-based adjustment scheme is adopted [28], as shown in (29)-(31). Equation (29) expresses that the output power adjustments of NGUs and GUs are equal to reserve participation factors (RPFs) multiplying the total deviation of RGUs and electrical loads. RPFs of NGUs and GUs are continuous variables between 0 and 1 as (30). To mitigate power deviation totally, the sum of RPFs at each period is equal to 1 as (31).

$$\Delta p_{ut} = -\alpha_{ut} \left(\sum_{u_R \in \mathcal{U}_R} \Delta \tilde{p}_{u_R t} - \sum_{d_e \in \mathcal{D}_e} \Delta \tilde{p}_{d_e t} \right) \quad \forall u, \forall t \quad (29)$$

$$0 \leq \alpha_{ut} \leq 1 \quad \forall u, \forall t \quad (30)$$

$$\sum_{u \in \mathcal{U}_N \cup \mathcal{U}_G} \alpha_{ut} = 1 \quad \forall t \quad (31)$$

Similarly, the deviations of gas loads with respect to predicted values need to be mitigated in real-time operation of the gas network, which are mitigated by the local GSs in this work [20]. Therefore, their input and output flows would be adjusted according to (32). Since GSs serve as the sole adjustable resources, the deviations of gas loads must be mitigated totally by local GSs, and the GSs must be equipped in each node connected to gas loads.

$$\Delta f_{st}^{out} - \Delta f_{st}^{in} = \sum_{d_g \in \mathcal{D}_g(s)} \Delta \tilde{f}_{d_g t} + \sum_{u_G \in \mathcal{U}_G(s)} \frac{\Delta \tilde{p}_{u_G t}}{\eta_{u_G t}} K \quad \forall s, \forall t \quad (32)$$

D. Equivalent Counterpart of Constraint with Random Variable

In constraints (5)-(28), the random variables are introduced, making the overall model intractable. In this regard, robust equivalent constraints of IEGS are proposed as (33)-(39) and (40)-(46) to replace (9)-(14) and (24)-(26) [29], respectively.

Based on LDR, the power balance of the whole power network can be satisfied. Formulae (33)-(37) are imposed to

preserve enough regulation capacity for the controllable units, which are the minimum requirements for URs and DRs by (33) and (34), base-case unit output ranges considering reserves by (35), and the worst-case ramping constraints by (36) and (37).

$$r_{ut}^{up} \geq \alpha_{ut} \left(\sum_{d_e \in \mathcal{D}_e} \Delta P_{d_e t}^{max} - \sum_{u_R \in \mathcal{U}_R} \Delta P_{u_R t}^{min} \right) \quad \forall u, \forall t \quad (33)$$

$$r_{ut}^{down} \geq \alpha_{ut} \left(\sum_{u_R \in \mathcal{U}_R} \Delta P_{u_R t}^{max} - \sum_{d_e \in \mathcal{D}_e} \Delta P_{d_e t}^{min} \right) \quad \forall u, \forall t \quad (34)$$

$$P_u^{min} + r_{ut}^{down} \leq p_{ut} \leq P_u^{max} - r_{ut}^{up} \quad \forall u, \forall t \quad (35)$$

$$(p_{ut} + r_{ut}^{up}) - (p_{u(t-1)} - r_{u(t-1)}^{down}) \leq R e_u^{up} \quad \forall u, \forall t \quad (36)$$

$$-R e_u^{down} \leq (p_{ut} - r_{ut}^{down}) - (p_{u(t-1)} + r_{u(t-1)}^{up}) \quad \forall u, \forall t \quad (37)$$

Further, (38) and (39) give the transmission line capacity constraints for the redistributed power flow considering the uncertainties as well as the active adjustments of nodal injections.

$$-P_{l_e}^{max} \leq p_{l_e t} + \sum_{u_R \in \mathcal{U}_R} \phi_{l_e u_R t} + \sum_{d_e \in \mathcal{D}_e} \phi_{l_e d_e t} \leq P_{l_e}^{max} \quad \forall l_e, \forall t \quad (38)$$

$$\begin{cases} p_{l_e t}^0 + \sum_{u_R \in \mathcal{U}_R} \phi_{l_e u_R t} + \sum_{d_e \in \mathcal{D}_e} \phi_{l_e d_e t} \leq P_{l_e}^{max} & \forall l_e, \forall t \\ -p_{l_e t}^0 + \sum_{u_R \in \mathcal{U}_R} \phi'_{l_e u_R t} + \sum_{d_e \in \mathcal{D}_e} \phi'_{l_e d_e t} \leq P_{l_e}^{max} & \forall l_e, \forall t \\ \phi_{l_e u_R t} \geq \Delta P_{u_R t}^{max} \left(G_{u_R l_e} - \sum_{u \in \mathcal{U}_N \cup \mathcal{U}_G} G_{u l_e} \alpha_{ut} \right) & \forall l_e, \forall u_R, \forall t \\ \phi_{l_e u_R t} \geq \Delta P_{u_R t}^{min} \left(G_{u_R l_e} - \sum_{u \in \mathcal{U}_N \cup \mathcal{U}_G} G_{u l_e} \alpha_{ut} \right) & \forall l_e, \forall u_R, \forall t \\ \phi'_{l_e u_R t} \geq -\Delta P_{u_R t}^{max} \left(G_{u_R l_e} - \sum_{u \in \mathcal{U}_N \cup \mathcal{U}_G} G_{u l_e} \alpha_{ut} \right) & \forall l_e, \forall u_R, \forall t \\ \phi'_{l_e u_R t} \geq -\Delta P_{u_R t}^{min} \left(G_{u_R l_e} - \sum_{u \in \mathcal{U}_N \cup \mathcal{U}_G} G_{u l_e} \alpha_{ut} \right) & \forall l_e, \forall u_R, \forall t \\ \phi_{l_e d_e t} \geq -\Delta P_{d_e t}^{max} \left(G_{d_e l_e} - \sum_{u \in \mathcal{U}_N \cup \mathcal{U}_G} G_{u l_e} \alpha_{ut} \right) & \forall l_e, \forall d_e, \forall t \\ \phi_{l_e d_e t} \geq -\Delta P_{d_e t}^{min} \left(G_{d_e l_e} - \sum_{u \in \mathcal{U}_N \cup \mathcal{U}_G} G_{u l_e} \alpha_{ut} \right) & \forall l_e, \forall d_e, \forall t \\ \phi'_{l_e d_e t} \geq \Delta P_{d_e t}^{max} \left(G_{d_e l_e} - \sum_{u \in \mathcal{U}_N \cup \mathcal{U}_G} G_{u l_e} \alpha_{ut} \right) & \forall l_e, \forall d_e, \forall t \\ \phi'_{l_e d_e t} \geq \Delta P_{d_e t}^{min} \left(G_{d_e l_e} - \sum_{u \in \mathcal{U}_N \cup \mathcal{U}_G} G_{u l_e} \alpha_{ut} \right) & \forall l_e, \forall d_e, \forall t \end{cases} \quad (39)$$

Since gas flow deviations are mitigated by the local GSs, the nodal gas flow balancing constraint can always be satisfied. Robust equivalent constraints of GSs are described by (40)-(46). Specifically, (40) and (41) are imposed to limit input and output flows of GSs in the worst case, (42) and (43) are added to guarantee the adequacy of worst-case available

gas, (44) depicts the temporal variation of the stored gas, and (45) and (46) express the uncertainty interval of gas loads.

$$0 \leq f_{st}^{in} \leq F_{s,max}^{in} + \Delta f_{st}^{min} \quad \forall s, \forall t \quad (40)$$

$$0 \leq f_{st}^{out} \leq F_{s,max}^{out} - \Delta f_{st}^{max} \quad \forall s, \forall t \quad (41)$$

$$s_s - \sum_{t'=1}^t \Delta f_{st'}^{min} \eta_s^{in} \leq s_s^{max} \quad \forall s, \forall t \quad (42)$$

$$s_s^{min} \leq s_s - \sum_t \frac{\Delta f_{st}^{max}}{\eta_s^{out}} \quad \forall s, \forall t \quad (43)$$

$$s_s^{min} \leq s_{st} = s_{s(t-1)} + f_{st}^{in} \eta_s^{in} - \frac{f_{st}^{out}}{\eta_s^{out}} \leq s_s^{max} \quad \forall s, \forall t \quad (44)$$

$$\Delta f_{st}^{min} = \sum_{d_g \in \mathcal{D}_g(s)} \Delta F_{d_g,t}^{min} - \sum_{u_g \in \mathcal{U}_g(s)} \frac{r_{u_g,t}^{down}}{\eta_{u_g}} K \quad \forall s, \forall t \quad (45)$$

$$\Delta f_{st}^{max} = \sum_{d_g \in \mathcal{D}_g(s)} \Delta F_{d_g,t}^{max} + \sum_{u_g \in \mathcal{U}_g(s)} \frac{r_{u_g,t}^{up}}{\eta_{u_g}} K \quad \forall s, \forall t \quad (46)$$

III. SOLUTION METHODOLOGY

Due to the existence of the nonconvex Weymouth equation (17), the proposed robust energy management model for the R-IEGS is not readily imported to the decentralized solution algorithm. In this section, the approximation and feasibility recovery methods for the Weymouth equation will be firstly introduced, and then the details of the adopted decentralized solution algorithm will be elaborated. This section ends with the description of the overall solution procedure. For the ease of analysis, the robust energy management problem for an R-IEGS, namely P1.

$$P1: \begin{cases} (1) \\ \text{s.t. (5)-(8), (15)-(23), (30), (31), (33)-(46)} \end{cases} \quad (47)$$

A. Linear Approximation for Weymouth Equation

According to (16) and (17), the relationship between the gas flow in a pipeline and the pressure square difference across the pipeline, denoted as $\Delta \tau_{l_p,t}$ is drawn in Fig. 1 and termed the Weymouth curve AB . In gas network, the lower and upper bounds of nodal pressure may be different, leading to asymmetry of the Weymouth curve with respect to the origin. Note that $f_{l_p,t}^*$ and $f_{l_p,t}^{**}$ are the positive and negative flow quantities of pipeline, respectively; $\Delta \tau_{l_p,t}^{*I}$ and $\Delta \tau_{l_p,t}^{*II}$ are the corresponding pressure square deviations of positive flow quantities under P1 and P2, respectively; $\Delta \tau_{l_p,t}^{**I}$ and $\Delta \tau_{l_p,t}^{**II}$ are the corresponding pressure square deviations of negative flow quantities under P1 and P2, respectively.

To construct a reasonable and tractable approximation for the Weymouth equation, an extension of the Weymouth curve in the third quadrant of Fig. 1 is performed to make it a symmetric one as AC . Then, we connect points A and C with a straight line, named the approximation curve, and it will go through the origin due to the symmetry of the two points. The expression of the approximation curve can be derived as (48).

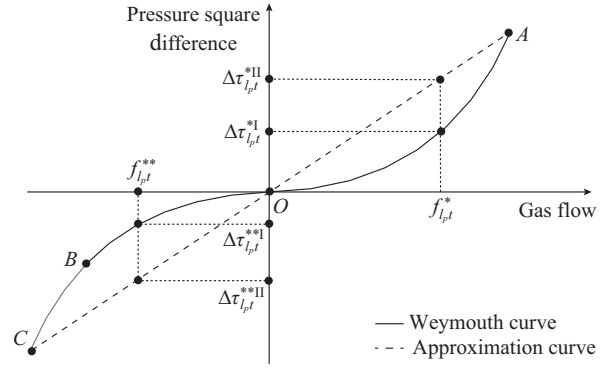


Fig. 1. Geometric interpretation of Weymouth equation and its approximation.

$$\tau_{l_p,t}^+ - \tau_{l_p,t}^- = \sqrt{\frac{\max(\tau_{l_p,t}^{max} - \tau_{l_p,t}^{min}, \tau_{l_p,t}^{max} - \tau_{l_p,t}^{min})}{\psi_{l_p}}} f_{l_p,t} \quad \forall l_p, \forall t \quad (48)$$

In this regard, we replace Weymouth equation (17) with its approximation (48) and preserve other constraints of P1, resulting in a linear approximation for P1, denoted as P2, which is a quadratic programming problem with linear constraints. Its compact form is introduced in (49).

$$P2: \begin{cases} \min \{ \mathbf{Q}^T \mathbf{x} \mathbf{Q} + \mathbf{q}^T \mathbf{x} + \mathbf{r} \} \\ \text{s.t. } \mathbf{A} \mathbf{x} \leq \mathbf{b} \end{cases} \quad (49)$$

\mathbf{Q} , \mathbf{q} , and \mathbf{r} can be derived from objective function (1); and \mathbf{A} and \mathbf{b} can be obtained from linear constraints (5)-(8), (15), (16), (18)-(23), (30), (31), (33)-(46), and (48).

The approximation error of P2 exists inevitably, which is illustrated in Fig. 1. Supposing the gas flow is known as $f_{l_p,t}^* \geq 0$, the corresponding pressure square differences of P1 and P2 can be obtained based on (17) and (48), denoted as $\Delta \tau_{l_p,t}^{*I}$ and $\Delta \tau_{l_p,t}^{*II}$, respectively. Intuitively, (50) can be obtained, which can be observed from Fig. 1.

$$\Delta \tau_{l_p,t}^{*I} \leq \Delta \tau_{l_p,t}^{*II} \quad f_{l_p,t}^* \geq 0, \forall l_p, \forall t \quad (50)$$

In fact, considering the asymmetry of the Weymouth and the approximation curves, a stronger conclusion would be drawn if $f_{l_p,t}^{**} < 0$, which is:

$$|\Delta \tau_{l_p,t}^{*I}| < |\Delta \tau_{l_p,t}^{*II}| \quad f_{l_p,t}^{**} < 0, \forall l_p, \forall t \quad (51)$$

From (50) and (51), it can be inferred that P2 requires larger pressure differences to maintain the same gas flows as P1 in most occasions (two exceptions are point A and the origin in Fig. 1, where the pressure differences are the same).

It should be noted that the pressure square difference $\Delta \tau_{l_p,t}$ in Fig. 1 is a linear combination of two independent variables, i.e., $\tau_{l_p,t}^+$ and $\tau_{l_p,t}^-$. The impacts of the proposed approximated model on the feasible region of the nodal pressure square variables $\tau_{l_p,t}^+$ and $\tau_{l_p,t}^-$ are demonstrated in Fig. 2.

Figure 2 includes two circumstances of the pressure mapping of the initial and terminal nodes with a predetermined gas flow, where the gas flow takes positive and negative values, respectively. Specially, $\Delta_{l_p,t}^*(\Delta_{l_p,t}^{**})$ and $\Delta_{l_p,t}^*(\Delta_{l_p,t}^{**})$ express the reduced feasible intervals of the pressure square of the initial and terminal nodes of a pipeline, respectively, when the gas

flow direction is positive (negative). From Fig. 2, it can be observed that the pressure square feasible intervals of the initial and terminal nodes would decrease if the Weymouth equation (17) is approximated by (48), regardless of the flow direction, leading to a smaller feasible region for the overall problem. On this account, if P2 has a solution, it must be a feasible (may be suboptimal) solution of P1. However, even if P1 is feasible, P2 can be either feasible or infeasible.

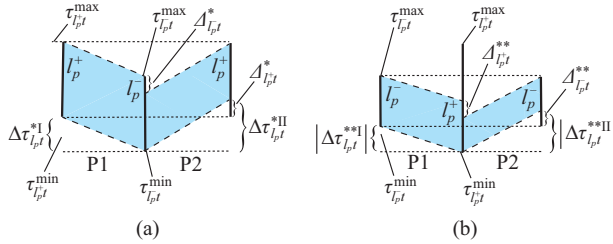


Fig. 2. Comparison of feasible regions of P1 and P2. (a) Positive gas flow direction. (b) Negative gas flow direction.

To cope with the shrinkage of feasible region in P2, a coarser but still linear approximation for P1 is proposed, where (16) is removed directly without introducing any substitute, and is denoted as P3, whose compact form is introduced in (52).

$$P3: \begin{cases} \min \{Q^T x Q + q^T x + r\} \\ \text{s.t. } A^* x \leq b^* \end{cases} \quad (52)$$

A^* and b^* can be obtained from linear constraints (5)-(8), (15), (18)-(23), (30), (31), (33)-(46), and (48). The only difference between P2 and P3 is that the nodal pressure constraint (16) is neglected in P3. Obviously, the feasible region of P3 is larger than that of P1, as the values of nodal pressures are not constrained.

From the perspective of the physical meaning, the transmission capacity of the pipeline is determined by its initial and terminal pressure limits. Thus, the transmission capacity of the pipeline in P1 is larger than P2, since the absolute values of pressure differences in P2 under the same gas flow are larger than those in P1 [22]. When the limit of nodal pressure square is neglected, the transmission capacity of the pipeline would be expanded in P3. In the devised overall solution procedure, P2 and P3 would be solved sequentially to determine the gas flow directions and initial gas flow, the details of which can be found at the end of Section III. Through the combination of P2 and P3, the optimal or at least a feasible solution can be obtained.

B. Feasibility Recovery

Though P2 or P3 can provide approximate solutions at relatively low computation costs, the solutions cannot reflect the actual nodal pressures of the gas network. Hence, additional treatment is adopted to amend the pressure deviations so as to recover a feasible solution of the physically meaningful P1. Based on the gas flow of pipeline obtained by P2 or P3, gas flow directions can be determined, and the Weymouth equation can be simplified as:

$$f_{l_p}^2 = \psi_{l_p} (\tau_{l_p^+} - \tau_{l_p^-}) \quad \forall l_p, \forall t \quad (53)$$

For the sake of simplicity, the flow direction is assumed to be the same as the positive direction of the pipeline.

Then, (53) can be replaced by a pair of opposite inequalities:

$$\psi_{l_p} (\tau_{l_p^+} - \tau_{l_p^-}) - f_{l_p}^2 \geq 0 \quad \forall l_p, \forall t \quad (54)$$

$$f_{l_p}^2 - \psi_{l_p} (\tau_{l_p^+} - \tau_{l_p^-}) \geq 0 \quad \forall l_p, \forall t \quad (55)$$

Formula (54) is convex quadratic. According to [15], the concave region defined as (55) can be tackled by the P-CCP proposed in [30] with an initial value of the gas flow. The details of the P-CCP can be seen in Algorithm 1 [15]. Formula (56) is introduced to replace (55) based on the initial gas flow of the pipeline obtained by P2 or P3, and penalty term related to slack variable is added to the objective function in (57). Thus, P4 is established and solved iteratively in Algorithm 1.

$$2f_{l_p}^0 f_{l_p} - (f_{l_p}^0)^2 - \psi_{l_p} (\tau_{l_p^+} - \tau_{l_p^-}) \geq \zeta_{l_p}^k, \quad \zeta_{l_p}^k \geq 0, \quad \forall l_p, \forall t \quad (56)$$

$$P4: \begin{cases} \min_{x, \zeta} \text{Obj}_i^k = \text{Cost}_i + \sigma_k \sum_{i \in \mathcal{T}} \sum_{l_p \in \mathcal{L}_p} \zeta_{l_p}^k \\ \text{s.t. (5)-(8), (15), (16), (18)-(23)} \\ \quad (30), (31), (33)-(46), (54), (56) \end{cases} \quad (57)$$

Algorithm 1: P-CCP for feasibility recovery

Step 1: set the values of $\kappa, \sigma_0, \text{Obj}_i^0, k_{\max}, \sigma_{\max}$; set the convergence tolerance $\delta = 0.1, \varepsilon = 10^{-4}$, iteration index $k = 0$.

Step 2: according to the solution of P2 or P3, obtain the gas flow directions and initial gas flows $f_{l_p}^0$.

Step 3: linearize the convex-concave inequality (55) with (56); solve P4.

Step 4: check the convergence residuals by (58) and (59). If both (58) and (59) are met, then exit; else if $k = k_{\max}$, then exit; else set $k = k + 1$, $\sigma_k = \min(\kappa \sigma_{k-1}, \sigma_{\max})$; set the obtained gas flow as the new initial value $f_{l_p}^0$, and return to *Step 3*.

$$|\text{Obj}_i^k - \text{Obj}_i^{k-1}| \leq \delta \quad (58)$$

$$\zeta_{l_p}^k \leq \varepsilon \left| 2f_{l_p}^0 f_{l_p} - (f_{l_p}^0)^2 \right| \quad \forall l_p, \forall t \quad (59)$$

Note that when the flow direction is opposite, the feasibility recovery method is similar.

C. Solution Coordination Among R-IEGS

The robust energy management problem for M-IEGS can be depicted as (60) and can be separated into sub-problems of areas by ADMM, whose details are described in Algorithm 2 [8], [18].

$$\begin{cases} \min \sum_{i \in \mathcal{A}} \text{Cost}_i(x_i) \\ \text{s.t. } x_i \in \Omega_i \quad \forall i \\ \quad A_e x_i + B_e x_j = c_e \quad \forall i, \forall j \in \mathcal{A}_i^e \\ \quad A_g x_i + B_g x_j = c_g \quad \forall i, \forall j \in \mathcal{A}_i^g \end{cases} \quad (60)$$

$A_e, B_e, c_e, A_g, B_g, c_g$ are derived from (27) and (28). The augmented Lagrangian function for R-IEGS i is:

$$L(x_i) = \min_{x_i \in \Omega_i} \left\{ \text{Cost}_i(x_i) + \sum_{j \in \mathcal{A}_i^e} \left[\lambda_e^T (A_e x_i + B_e x_j - c_e) + \frac{d_e}{2} \|A_e x_i + B_e x_j - c_e\|^2 \right] + \sum_{j \in \mathcal{A}_i^g} \left[\lambda_g^T (A_g x_i + B_g x_j - c_g) + \frac{d_g}{2} \|A_g x_i + B_g x_j - c_g\|^2 \right] \right\} \quad (61)$$

Algorithm 2: ADMM for M-IEGSs

Step 1: initialize the value of x_p^0 , λ_e^0 and λ_g^0 , set the convergence tolerance value $\varepsilon^{abs} = 10^{-4}$, $\varepsilon^{rel} = 4 \times 10^{-3}$, iteration index $k = 0$.

Step 2: solve (61) for all the R-IEGSs and update λ_e^k and λ_g^k by:

$$\lambda_e^{k+1} = \lambda_e^k + d_e (A_e x_i^k + B_e x_j^k - c_e) \quad (62)$$

$$\lambda_g^{k+1} = \lambda_g^k + d_g (A_g x_i^k + B_g x_j^k - c_g) \quad (63)$$

Step 3: check the convergence residuals of each area by (64). The tolerances of primal and dual residuals ε^{pri} and ε^{dual} can be calculated by ε^{abs} and ε^{rel} , respectively [8]. If (64) holds, terminates; else set $k = k + 1$ and return to Step 2.

$$\begin{cases} \|A_e x_i^k + B_e x_j^k - c_e\|_2 \leq \varepsilon^{pri} \\ \|d_e A_e^T B_e (x_j^{k+1} - x_j^k)\|_2 \leq \varepsilon^{dual} \\ \|d_g A_g^T B_g (x_j^{k+1} - x_j^k)\|_2 \leq \varepsilon^{dual} \end{cases} \quad (64)$$

D. Acceleration Strategy

Though all the proposed models are convex, the potential computation burden is still huge considering the auxiliary constraints generated during constraint robustification, especially for the power flow security constraints (39). Therefore, an acceleration strategy is designed to ease the computation burden in the proposed model.

In most cases, all the decision variables except nodal pressure are unchanged after amendment, which suggests the solution of P3 is a feasible solution of P1. Therefore, gas pressure deviation can be amended in gas network locally with the fixed input and output of gas network. The solved problem is shown in (65), namely P5. Based on this, the acceleration scheme is to replace P4 with P5 in Algorithm 1. In this case, the robust power network constraints can be removed from the feasibility recovery process, suggesting remarkable decrement of the solution time.

P5:

$$\begin{aligned} \min O_i^k = & \sum_{t \in \mathcal{T}} \left[\sum_{p \in \mathcal{L}_p} \sigma_k \zeta_{p,t}^k + \sum_{w \in \mathcal{W}} (\Delta f_{wt}^+ + \Delta f_{wt}^-) + \right. \\ & \sum_{s \in \mathcal{S}} (\Delta f_{st}^+ + \Delta f_{st}^-) + \sum_{u_G \in \mathcal{L}_G} (\Delta p_{u_G,t}^+ + \Delta p_{u_G,t}^-) + \sum_{j \in \mathcal{A}_i^g} (\Delta f_{t,j}^{+,+} + \Delta f_{t,j}^{+,-}) + \\ & \left. \sum_{u_G \in \mathcal{L}_G} (\Delta r_{u_G,t}^{up,+} + \Delta r_{u_G,t}^{up,-} + \Delta r_{u_G,t}^{down,+} + \Delta r_{u_G,t}^{down,-}) \right] \end{aligned} \quad (65)$$

s.t. (15), (16), (18)-(23), (40)-(46), (54), (56)

$$f_{wt} = f_{wt}^{III} + \Delta f_{wt}^+ - \Delta f_{wt}^- \quad \forall w, \forall t \quad (66)$$

$$f_{st}^{out} - f_{st}^{in} = f_{st}^{out,III} - f_{st}^{in,III} + \Delta f_{st}^+ - \Delta f_{st}^- \quad \forall s, \forall t \quad (67)$$

$$p_{u_G,t} = p_{u_G,t}^{III} + \Delta p_{u_G,t}^+ - \Delta p_{u_G,t}^- \quad \forall u_G, \forall t \quad (68)$$

$$f_{t,j} = f_{t,j}^{III} + \Delta f_{t,j}^{+,+} - \Delta f_{t,j}^{+,-} \quad \forall j \in \mathcal{A}_i^g, \forall t \quad (69)$$

$$r_{u_G,t}^{up} = r_{u_G,t}^{up,III} + \Delta r_{u_G,t}^{up,+} - \Delta r_{u_G,t}^{up,-} \quad \forall u_G, \forall t \quad (70)$$

$$r_{u_G,t}^{down} = r_{u_G,t}^{down,III} + \Delta r_{u_G,t}^{down,+} - \Delta r_{u_G,t}^{down,-} \quad \forall u_G, \forall t \quad (71)$$

$$\Delta f_{wt}^+, \Delta f_{wt}^-, \Delta f_{st}^+, \Delta f_{st}^-, \Delta p_{u_G,t}^+, \Delta p_{u_G,t}^-, \Delta f_{t,j}^{+,+}, \Delta f_{t,j}^{+,-} \geq 0 \quad (72)$$

$$\Delta r_{u_G,t}^{down,+}, \Delta r_{u_G,t}^{down,-}, \Delta r_{u_G,t}^{up,+}, \Delta r_{u_G,t}^{up,-} \geq 0 \quad (73)$$

where the symbols with prefix Δ^+ , Δ^- and superscript III represent the positive and negative slack variables and the solu-

tion from P3, respectively.

In some cases, the solution of P3 is infeasible with respect to P1, and nearly all the decision variables would be changed after amendment. At this moment, the proposed acceleration scheme is ineffective, and the nodal pressure deviation must be amended by solving P4. Therefore, the problem is how to judge whether the solution of P3 is feasible for P1 or not. First, the solution of P3 is assumed feasible for P1. Then, P5 is solved by Algorithm 1. If the objective of P5 is beyond the threshold after the convergence of Algorithm 1, the pressure deviation cannot be mitigated locally in the gas network, and the proposed acceleration scheme is ineffective, then P5 would be adopted in Algorithm 1. However, if the objective of P5 becomes smaller than the threshold during the execution of Algorithm 1, the pressure deviation can be solved by the gas network and certain computation time can be saved. It should be noted that the proposed acceleration scheme would not influence the optimality of the solution as the variables related with the objective function of the original model have been fixed as constants.

E. Overall Solution Procedure

The flowchart of the overall solution procedure is demonstrated in Fig. 3. Firstly, all the R-IEGSs would participate in Algorithm 2 to solve P3 locally and the gas flow directions can be obtained. Then, the feasibility of the solution with respect to the unrelaxed constraints is recovered by solving P5 and P4 sequentially. Considering that the feasible region of P3 is larger than that of P1, the gas flow direction obtained by P3 may be infeasible, resulting in the convergence failure of Algorithms 1 and 2. Therefore, P2 would be solved to modify the gas flow directions, and the feasibility of the solution would be recovered by solving P4. Because of the shrinkage of feasible region in P2, the gas flow directions obtained by P2 must be feasible, avoiding the convergence failure caused by the infeasible gas flow directions.

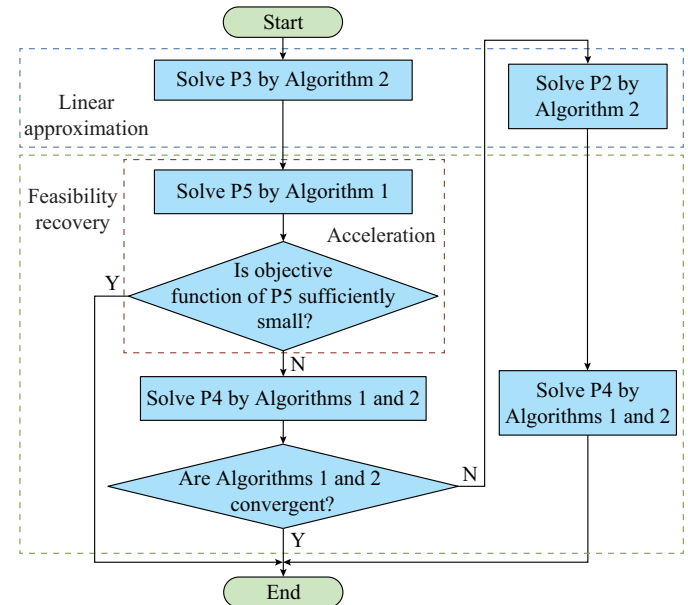


Fig. 3. Flowchart of overall solution procedure.

Noted that only convex programs are solved in Fig. 3, which not only provides theoretical guarantee for the convergence of Algorithms 1 and 2 but also suggests acceptable computation burden for large-scale test systems. In order to clarify the differences of the five proposed models, the details of the five models are gathered in Table II, where the last two columns show the exclusive constraints and their descriptions. Concretely, P1 is the original problem, which is an NLP. P2 and P3 are approximations of P1 to obtain the gas flow direc-

tions and initial gas flow. Both P4 and P5 are used to eliminate the impacts of linear approximation on solution feasibility, whose prominent characteristic is using two convex equations (54) and (56) to replace the Weymouth equation. The difference between P2 and P3 lies in the existence of nodal pressure constraint (16), reflecting the feasible region difference of two programs. The difference between P4 and P5 is whether the input and output of the gas network are fixed or not.

TABLE II
COMPARISON OF FIVE PROPOSED MODELS

Model	Description	Mathematical property	Shared constraint	Exclusive constraint	Description of exclusive constraint
P1	Original problem	Non-linear programming	(15), (18)-(23), (30)-(31)	(5)-(8), (33)-(39)	Power network constraints
				(16)	Nodal pressure constraint
				(17)	Weymouth equation constraint
P2	Linear approximation	Quadratic programming with linear constraint		(5)-(8), (33)-(39)	Power network constraints
				(16)	Nodal pressure constraint
				(48)	Linearized Weymouth equation constraint
P3	Linear approximation	Quadratic programming with linear constraint		(5)-(8), (33)-(39)	Power network constraints
				(48)	Linearized Weymouth equation constraint
P4	Feasibility recovery of linear approximation	Quadratic programming with SOC constraint		(5)-(8), (33)-(39)	Power network constraints
				(16)	Nodal pressure constraint
				(54)	SOC constraint of Weymouth equation
				(56)	Constraint added by P-CCP
				(16)	Nodal pressure constraint
P5	Feasibility recovery by acceleration strategy	Linear programming with SOC constraint		(54)	SOC constraint of Weymouth equation
				(56)	Constraint added by P-CCP
				(66)-(73)	Constraints used to fix the inputs and outputs of gas network

IV. CASE STUDY

In this section, the performances of the proposed linear approximations as well as the acceleration scheme are justified by several different gas networks and single R-IEGS of different scales. Then, the proposed methods are first implemented on a small-scale M-IEGS to validate the effectiveness, whose topology is depicted in Fig. 4. At last, the results of scalability tests for the proposed methods are demonstrated. All the parameters and topologies of all test systems in detail can be seen in [31].

The test system depicted in Fig. 4 consists of two R-IEGSs, denoted as R-IEGS I and R-IEGS II, respectively. R-IEGS I includes a 5-bus power network and a 7-node gas network, and R-IEGS II incorporates a 6-bus power network and a 6-node gas network. The two R-IEGSs are interconnected through a DC tie-line and a gas tie-pipeline, which are depicted through the point lines.

A. Performance of LP-based Approximation Method

To test the performances of the proposed LP-based approximation methods for the Weymouth equations, the results of P2 and P3 in three gas networks are compared with the results of P1, which are solved by the IPOPT solver of OPTI toolbox. The results are demonstrated in Table III, where

G7, G10, and G20 are 7-node, 10-node, and 20-node gas networks, respectively. The topologies as well as related parameters of the test systems can be found in [31]. Specifically, the simulated models only incorporate operation constraints of the gas network so as to highlight the impacts of approximations on the Weymouth equations.

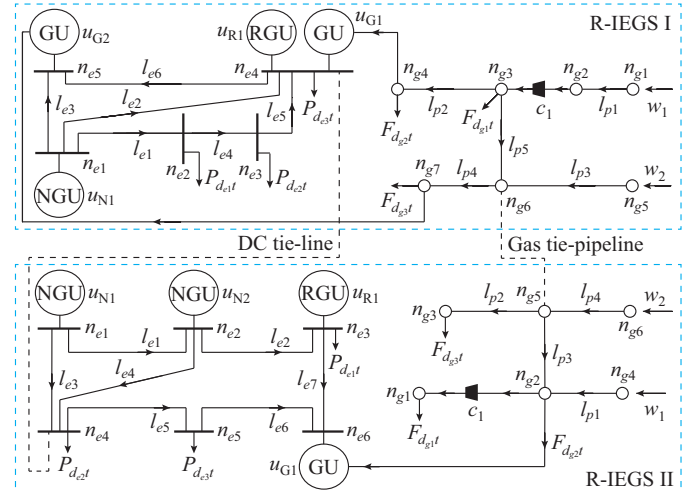


Fig. 4. Topology of two-area R-IEGS.

TABLE III
SIMULATION RESULTS OF P1-P3

Test system	P3		P2		Objective function of P1 (\$)
	Objective function (\$)	Sum of slack variable	Objective function (\$)	Sum of slack variable	
G7	6.2632×10^4	7.2943×10^{-14}	6.2632×10^4	7.2943×10^{-14}	6.2632×10^4
G10	1.4569×10^6	3.4835×10^{-9}	1.4569×10^6	3.6473×10^{-9}	1.4569×10^6
G20	1.3949×10^7	5.7857×10^{-7}	1.4247×10^7	1.9079×10^{-7}	1.3949×10^7

Noted that the solutions provided by IPOPT are always feasible in the three tests. In this regard, the last column of Table III is regarded as the benchmark. From Table III, it can be seen that the performances of the three models are the same for G7 and G10, in terms of the optimality and feasibility. For G20, P2 offers a 2.14% larger objective value than P1, while the solution feasibility with respect to the Weymouth equation is reached, which confirms P2 would cut off part of the feasible region of P1 and cause the increase of the objective. It should be observed that the solution quality of P3 is the same as P1 in the G20 case, which indicates P3 is a necessary supplement to P2. Noted that P3 is solved ahead of P2 in Algorithm 1, therefore, the proposed models can offer feasible solutions with good quality in all these three cases.

B. Effectiveness of Acceleration Technique

To validate the effectiveness of the designed acceleration technique, i.e., solving P5 instead of P4 using Algorithm 1 in the middle of the overall solution procedure, the computation performance of Algorithm 1 with P5 and P4 in 4 different R-IEGSs are presented in Table IV. The first column of Table IV indicates the size of the test system, e.g., P5-G7 representing a 5-bus power network integrated with a 7-node gas network. In each test system, the uncertainty intervals of the RGU outputs, electrical loads, and gas loads are 1%, 1%, and 0.1% of the predicted values, respectively. The topologies as well as the related parameters of the test systems can be found in [31].

TABLE IV
COMPUTATION PERFORMANCE OF ALGORITHM 1 UNDER P4 AND P5

Test system	P5		P4		Number of reduced constraints
	Time (s)	Iteration	Time (s)	Iteration	
P5-G7	0.245	1	0.334	1	3648
P6-G6	0.413	3	0.997	3	4152
P24-G10	3.791	1	1632.900	1	83712
P39-G20	1.972	1	365.200	2	100224

C. Strategy Robustness Test

In the proposed model, all the robust constraints are transformed into normal ones. To validate the effectiveness of the transformed model, one thousand scenarios are generated randomly. The uncertainty intervals of the RUs, electrical loads power, and gas loads are 15%, 10%, and 1.5% of the predicted values, respectively.

In power network, only one GU (u_{G1} in R-IEGS I) and one line (l_{e3} in R-IEGS I) are tested, and the result is shown

in Fig. 5. It can be observed that the power adjustment of GU falls between UR and DR, and the power flow is always below the capacity of the transmission line.

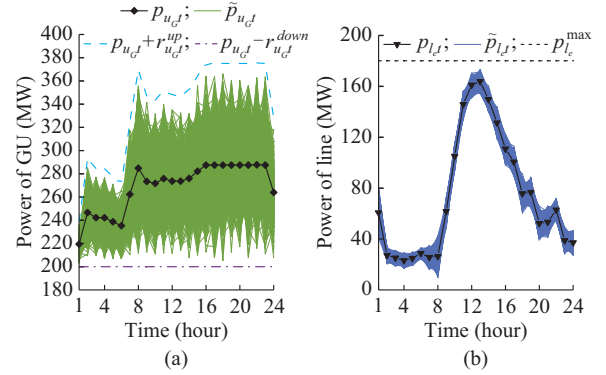


Fig. 5. Outputs of units and power flows in random cases. (a) Power of GU. (b) Power of line.

In gas network, only one GS (equipped in d_{g1} of R-IEGS I) is tested, and the result is shown in Fig. 6. Similarly, it can be viewed that the flow and adjustment of GS fall between the maximum and minimum values in all cases.

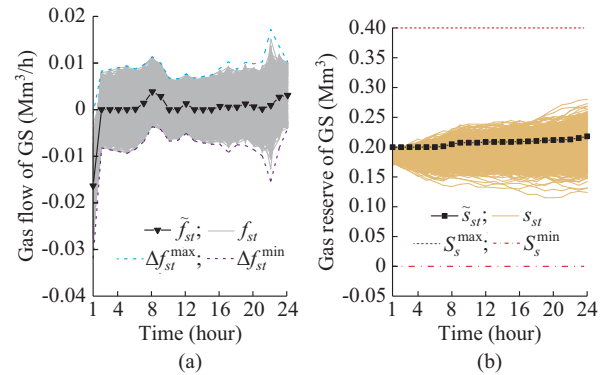


Fig. 6. Gas flow and reserve of GS in random cases. (a) Gas flow of GS. (b) Gas reserve of GS.

D. Comparison Among Different Gas Network Modeling Methods

To highlight the computation benefits of convex programming, some other solution methods for the decentralized robust energy management of M-IEGSs are implemented, including the IPOPT method (solving the nonlinear and non-convex P1 directly using the OPTI toolbox), and methods in [10] and [18]. The simulation results are summarized in Table V, where the term “Gap” indicates the difference of the left- and right-hand-side terms of the Weymouth equation

(17). It should be noted that the solution coordination among R-IEGSs is achieved by ADMM in all the listed methods, and the differences lie in the solution methods for the gas network models. Meanwhile, the intervals of the RGU outputs, electrical loads, and gas loads uncertainty are 1%, 1%, and 1%, respectively.

TABLE V
COMPARISON OF GAS NETWORK MODELING METHOD

Time period (hour)	Method	Model property	Objective (\$)	Gap (%)	Time (s)
2	IPOPT	NLP	1.7090×10^6	9.9920×10^{-6}	1.681
	[18]	MISOCP	1.7090×10^6	3.2758×10^{-4}	6.407
	[10]	MILP	1.7090×10^6	1.4800×10^0	2.759
	Proposed	SOCP	1.7090×10^6	4.3874×10^{-5}	1.231
6	IPOPT	NLP	5.5485×10^6	9.9976×10^{-6}	2.171
	[18]	MISOCP	5.5485×10^6	7.5831×10^{-4}	6.810
	[10]	MILP	5.5485×10^6	1.4800×10^0	54.823
	Proposed	SOCP	5.5485×10^6	3.9869×10^{-5}	1.822
12	IPOPT	NLP			
	[18]	MISOCP	1.0300×10^7	1.2252×10^{-2}	12.066
	[10]	MILP	1.0300×10^7	1.4800×10^0	217.058
	Proposed	SOCP	1.0300×10^7	1.7436×10^{-5}	1.845

From Table V, it can be observed that the proposed method can provide a good solution from the perspectives of optimality and feasibility in the shortest time. Among those, the performance of IPOPT is the worst, as it fails to generate a solution when $T=12$ hours. Moreover, the solutions of [10] cannot meet the feasibility requirement in three tests, as a trade-off between the computation burden and solution accuracy. When $T=12$ hours, the proposed method is almost 6

times faster than [18] and the solution quality is even better in terms of feasibility. Another observation is that the increment of computation time of the proposed method is the lowest among all these methods. The reason is that the computation burden of the method in [18] and [10] grows fast along with the growth of the period number, as the number of binary variables would grow accordingly, indicating the worse performance of the IPOPT and the methods in [18] and [10] in larger test systems as well as the necessity and significance of developing convex optimization based solution procedures.

E. Computation Efficiency Test

The proposed methods are performed on two larger test systems, denoted as TS-I and TS-II, whose parameters can be found in [31], so as to demonstrate the computation performance of the proposed methods on large-scale test systems. The components of TS-I and TS-II are listed in Table VI, where E118G48 means the R-IEGS is composed of a 118-bus power network and a 48-node gas network, and so on in a similar fashion. Here, times of computation burden (TCB) is defined as the ratio of the total number of constraints of the test system to that of the test system in Section IV-A with 24 time periods, which can reflect the computation burden increment. The simulation results are gathered in Table VI, where the column index ATPi is short for the average time per iteration.

From Table VI, it can be observed that the total computation time as well as ATPi grows almost linearly along with the number of periods in both test systems. For the day-ahead dispatch of the two test systems, the simulation time is within one hour and does not go up remarkably along with the system scale, which reveals the benefits of the proposed convex programming based solution procedure.

TABLE VI
COMPUTATION PERFORMANCE ON LARGE-SCALE TEST SYSTEM

Test system	System	Time period (hour)	TCB	Iteration	Total time (s)	ATPi (s)
Benchmark	E5G7-E6G6	24	1	7	1.859	0.266
		4	14	5	137.500	27.500
		8	29	5	263.100	52.600
		12	57	5	410.100	82.000
		16	86	5	559.400	111.900
TS-I	E39G20-E118G48	24	115	5	1012.400	202.500
		4	27	12	292.400	24.400
		8	55	12	517.900	43.200
		12	82	13	1065.100	81.900
		16	110	16	2390.500	183.900
TS-II	E24G10-E39G20-E118G48	24	165	15	3529.600	235.300

V. CONCLUSION

In this paper, a decentralized solution procedure for the robust energy management of M-IEGSs is proposed to mitigate the uncertainties from RGU outputs and energy demands. With the help of the LDR-based electrical reserve utilization scheme as well as the distributed GSs, a single-level

deterministic equivalence can be obtained for the non-trivial robust problem. A novel linear approximation method is proposed to tackle the nonconvexities brought by the Weymouth equations in gas networks, and the P-CCP is employed to recover the feasibility of approximate solutions with an acceleration strategy. The ADMM is adopted to realize a decen-

tralized computation of the robust energy management strategy. The overall solution procedure only requires solving convex optimizations, which provides convergence guarantee for the ADMM and P-CCP algorithms, and indicates good computation performances, especially for moderate test systems. The effectiveness of the linear approximations is verified by simulation results. It also can be observed that the proposed methods can provide an acceptable solution under the given time limit, especially for large-scale cases. The proposed methods are also suitable for addressing the locational marginal price-based market clearing problems of the M-IEGS, where convex programs are preferred.

REFERENCES

- [1] M. Shahidehpour, Y. Fu, and T. Wiedman. "Impact of natural gas infrastructure on electric power systems," *Proceedings of the IEEE*, vol. 93, no. 5, pp. 1042-1056, May 2005.
- [2] H. Sun, Q. Guo, B. Zhang *et al.*, "Integrated energy management system: concept, design, and demonstration in China," *IEEE Electrification Magazine*, vol. 6, no. 2, pp. 42-50, Jun. 2018.
- [3] G. Sun, S. Chen, Z. Wei *et al.*, "Multi-period integrated natural gas and electric power system probabilistic optimal power flow incorporating power-to-gas units," *Journal of Modern Power Systems and Clean Energy*, vol. 5, no. 3, pp. 412-423, May 2017.
- [4] L. Ni, W. Liu, F. Wen *et al.*, "Optimal operation of electricity, natural gas and heat systems considering integrated demand responses and diversified storage devices," *Journal of Modern Power Systems and Clean Energy*, vol. 6, no. 3, pp. 423-437, Jan. 2018.
- [5] J. Mi and M. E. Khodayar, "Operation of natural gas and electricity networks with line pack," *Journal of Modern Power Systems and Clean Energy*, vol. 7, no. 5, pp. 1056-1070, Sept. 2019.
- [6] S. Wang, Y. Ding, C. Ye *et al.*, "Reliability evaluation of integrated electricity-gas system utilizing network equivalent and integrated optimal power flow techniques," *Journal of Modern Power Systems and Clean Energy*, vol. 7, no. 6, pp. 1523-1535, Nov. 2019.
- [7] Z. Li, M. Shahidehpour, F. Aminifar *et al.*, "Networked microgrids for enhancing the power system resilience," *Proceedings of the IEEE*, vol. 105, no. 7, pp. 1289-1310, Jul. 2017.
- [8] S. Boyd, N. Parikh, E. Chu *et al.*, "Distributed optimization and statistical learning via the alternating direction method of multipliers," *Now Foundations and Trends*, vol. 3, no. 1, pp. 1-122, Jan. 2011.
- [9] Y. Liu, H. B. Gooi, and H. Xin. "Distributed energy management for the multi-microgrid system based on ADMM," in *Proceedings of 2017 IEEE PES General Meeting*, Chicago, USA, Jul. 2017, pp. 1-5.
- [10] C. M. Correa-Posada and P. Sanchez-Martin. (2014, Oct.). Gas network optimization: a comparison of piecewise linear models. [Online]. Available: http://www.optimization-online.org/DB_HTML/2014/10/4580.html
- [11] C. Correa-Posada and P. Sanchez-Martin, "Integrated power and natural gas model for energy adequacy in short-term operation," *IEEE Transactions on Power Systems*, vol. 30, no. 6, pp. 3347-3355, Jun. 2015.
- [12] C. He, L. Wu, T. Liu *et al.*, "Robust co-optimization scheduling of electricity and natural gas systems via ADMM," *IEEE Transactions on Sustainable Energy*, vol. 8, no. 2, pp. 658-670, Apr. 2017.
- [13] C. He, T. Liu, L. Wu *et al.*, "Robust coordination of interdependent electricity and natural gas systems in day-ahead scheduling for facilitating volatile renewable generations via power-to-gas technology," *Journal of Modern Power Systems and Clean Energy*, vol. 5, no. 3, pp. 375-388, Apr. 2017.
- [14] Y. He, M. Shahidehpour, Z. Li *et al.*, "Robust constrained operation of integrated electricity-natural gas system considering distributed natural gas storage," *IEEE Transactions on Sustainable Energy*, vol. 9, no. 3, pp. 1061-1071, Jul. 2018.
- [15] C. Wang, W. Wei, J. Wang *et al.*, "Convex optimization based distributed optimal gas-power flow calculation," *IEEE Transactions on Sustainable Energy*, vol. 9, no. 3, pp. 1145-1156, Jul. 2018.
- [16] C. Wang, W. Wei, J. Wang *et al.*, "Convex optimization based adjustable robust dispatch for integrated electric-gas systems considering gas delivery priority," *Applied Energy*, vol. 239, pp. 70-82, Apr. 2019.
- [17] S. Chen, A. Conejo, R. Sioshansi *et al.*, "Unit commitment with an enhanced natural gas-flow mode," *IEEE Transactions on Power Systems*, vol. 34, no. 5, pp. 3729-3738, Sept. 2019.
- [18] Y. He, M. Yan, M. Shahidehpour *et al.*, "Decentralized optimization of multi-area electricity-natural gas flows based on cone reformulation," *IEEE Transactions on Power Systems*, vol. 33, no. 4, pp. 4531-4542, Jul. 2018.
- [19] Y. Wen, X. Qu, W. Li *et al.*, "Synergistic operation of electricity and natural gas networks via ADMM," *IEEE Transactions on Smart Grid*, vol. 9, no. 5, pp. 4555-4565, Sept. 2018.
- [20] F. Liu, Z. Bie, and X. Wang, "Day-ahead dispatch of integrated electricity and natural gas system considering reserve scheduling and renewable uncertainties," *IEEE Transactions on Sustainable Energy*, vol. 10, no. 2, pp. 646-658, Apr. 2019.
- [21] C. He, L. Wu, T. Liu *et al.*, "Co-optimization scheduling of interdependent power and gas systems with electricity and gas uncertainties," *Energy*, vol. 159, pp. 1003-1015, Sept. 2018.
- [22] H. Cui, F. Li, Q. Hu *et al.*, "Day-ahead coordinated operation of utility-scale electricity and natural gas networks considering demand response based virtual power plants," *Applied Energy*, vol. 176, pp. 183-195, May 2016.
- [23] S. Chen, Z. Wei, G. Sun *et al.*, "Adaptive robust day-ahead dispatch for urban energy systems," *IEEE Transactions on Industrial Electronics*, vol. 66, no. 2, pp. 1379-1390, Feb. 2019.
- [24] L. Bai, F. Li, H. Cui *et al.*, "Interval optimization based operating strategy for gas-electricity integrated energy systems considering demand response and wind uncertainty," *Applied Energy*, vol. 167, pp. 270-279, Nov. 2015.
- [25] M. Mazidi, H. Monsef, and P. Siano. "Robust day-ahead scheduling of smart distribution networks considering demand response programs," *Applied Energy*, vol. 178, pp. 929-942, Jun. 2016.
- [26] Z. Li, M. Shahidehpour, W. Wu *et al.*, "Decentralized multiarea robust generation unit and tie-line scheduling under wind power uncertainty," *IEEE Transactions on Sustainable Energy*, vol. 6, no. 4, pp. 1377-1388, Oct. 2015.
- [27] Y. Li, C. Wang, G. Li *et al.*, "Improving operational flexibility of integrated energy system with uncertain renewable generations considering thermal inertia of buildings," *Energy Conversion and Management*, vol. 207, no. 1, p. 112526, Mar. 2020.
- [28] R. A. Jabr. "Adjustable robust OPF with renewable energy sources," *IEEE Transactions on Power Systems*, vol. 28, no. 4, pp. 4742-4751, Nov. 2013.
- [29] Z. Li, W. Wu, B. Zhang, *et al.* "Robust look-ahead power dispatch with adjustable conservativeness accommodating significant wind power integration," *IEEE Transactions on Sustainable Energy*, vol. 6, no. 3, pp. 781-790, Jul. 2015.
- [30] T. Lipp and S. Boyd. "Variations and extension of the convex-concave procedure," *Optimization and Engineering*, vol. 17, pp. 263-287, 2016.
- [31] C. Wang. (2020, Jan.). Data for decentralized robust optimization of M-IEGS. [Online]. Available: <https://sites.google.com/site/chengwang0617/home/data-sheet/robustm-ieg>

Nan Jia received the B.Sc. degree in the Department of Electrical Engineering, China University of Petroleum (East China), Qingdao, China, in 2018. He is currently pursuing the master degree with North China Electric Power University, Beijing, China. His research interest includes the decentralized robust optimization of integrated energy system.

Cheng Wang received the B.Sc. and Ph.D. degrees in electrical engineering from Tsinghua University, Beijing, China, in 2012 and 2017, respectively. He was a Visiting Ph.D. student with Argonne National Laboratory, Argonne, USA, from 2015 to 2016. He is currently an Associate Professor with North China Electric Power University, Beijing, China. His research interests include optimization and control of integrated energy systems.

Wei Wei received the B.Sc. and Ph.D. degrees in electrical engineering from Tsinghua University, Beijing, China, in 2008 and 2013, respectively. He was a Postdoctoral Research Fellow with Tsinghua University from 2013 to 2015. He was a Visiting Scholar with Cornell University, Ithaca, USA, in 2014, and with Harvard University, Cambridge, USA, in 2015. He is currently an Associate Professor with Tsinghua University. His research interests include applied optimization and energy economics.

Tianshu Bi received the Ph.D. degree at the Department of Electrical and Electronic Engineering in the University of Hong Kong, Hong Kong, China, in 2002. She is currently a Professor at North China Electric Power University, Beijing, China. Her research interests include power system protection and control, synchronized phasor measurement technique, and its application and fault diagnose.